

## Supplementary material

# Possible effects of anthropogenic and volcanic aerosols on the ITCZ and rainfall over South America

\*[1,2] Nicolás Duque-Gardeazabal; nicolas.duque@unibe.ch

[1,2] Stefan Brönnimann

[1,2,3] Andrew R. Friedman

[1,2] Jörg Franke

\*[1] Oeschger Centre for Climate Change Research, University of Bern, Bern, Switzerland

[2] Institute of Geography, University of Bern, Bern, Switzerland

[3] now at Laboratoire de Météorologie Dynamique / Institute Pierre-Simon Laplace, Paris, France

## Contents

<b>Supplementary Figures</b>	<b>2</b>
Figure S1 – Other hydroclimate anomalies in tropical South America . . . . .	2
Figure S2 – Meridional total energy transport in the 20th and 21st century . . . . .	3
Figure S3 – Global position of the strong ascent of moist air . . . . .	4
Figure S4 – Changes in Sea Level Pressure and low level winds . . . . .	5
Figure S5 – Early 19th century anomalies of the temperature contrast between the land and the ocean in the tropics . . . . .	6

## Supplementary Figures

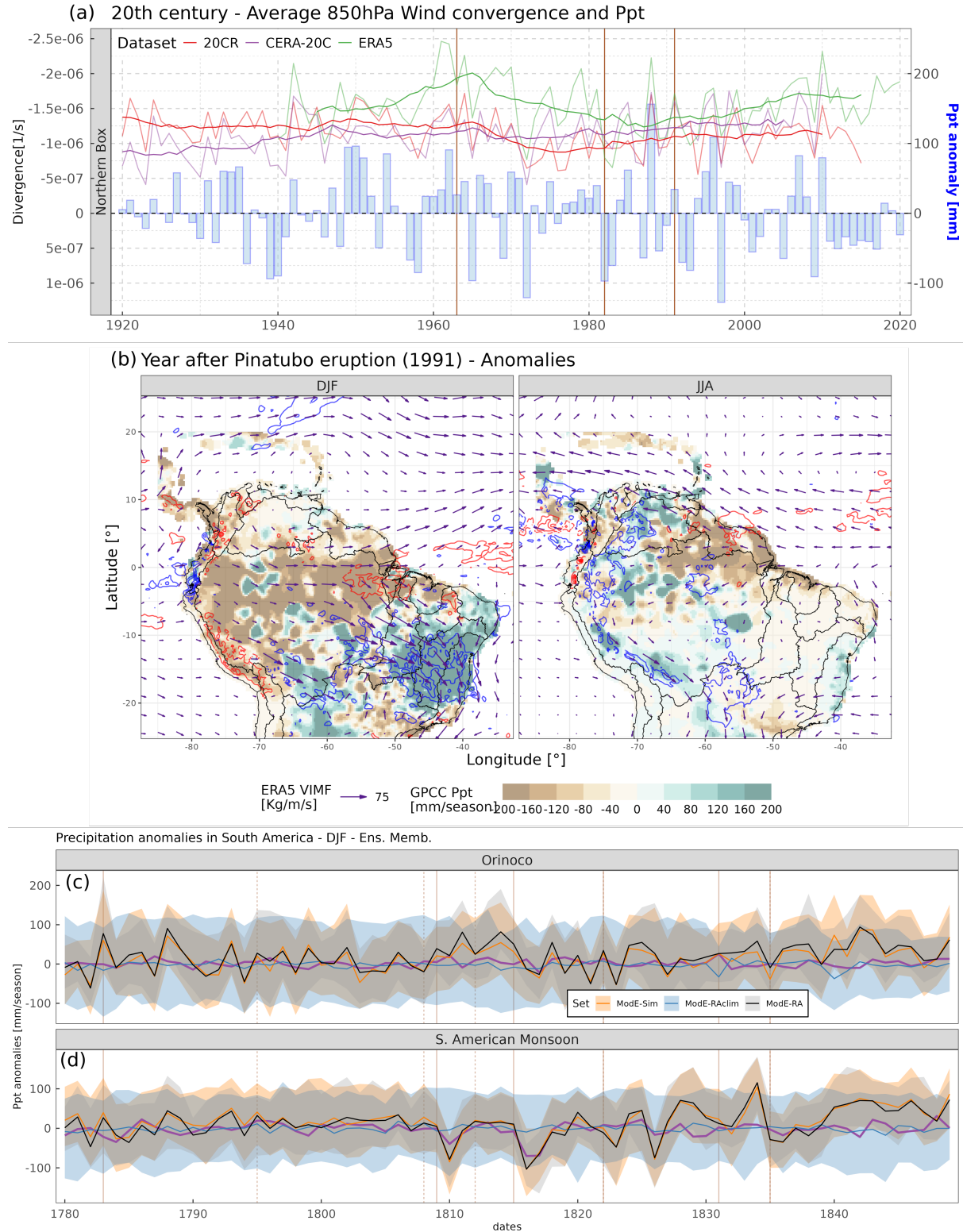


**Figure S1. Other hydroclimate anomalies in tropical South America** (a) Time series of JJA 850 hPa wind convergence and GPCC precipitation anomalies (right-side y-axis) in the northern box (Fig. 1a). (b) Anomalies of ERA5 VIMF (arrows), moisture divergence (contours) and GPCC precipitation (shading), in the year 1992 (year after mount Pinatubo's eruption). (c) and (d) Time series of precipitation anomalies in December to February for the northern and southern box (Fig. 1a) for the 19th century, using the ModE-RA reanalysis family. Lower and upper ribbon represent the 5 and 95 percentile ensemble members spread and tick color line the ensemble mean. Purple line depicts the CESM-LME ensemble mean. Vertical orange lines denote years with volcanic eruptions highlighted in Hand et al. (2023).

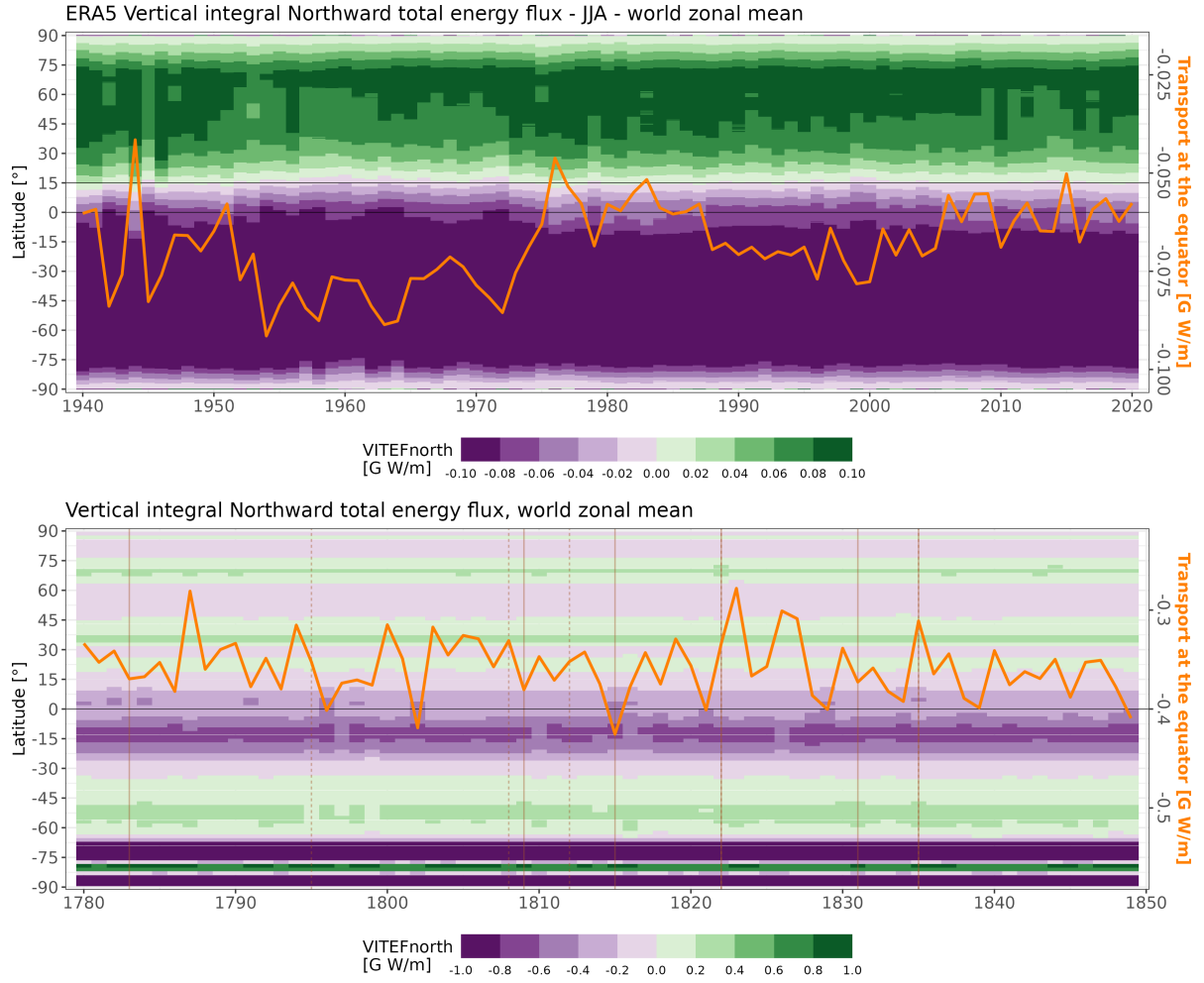


**Figure S2.** ERA5 meridional vertically integrated total energy flux in June to August for (top) the late 20th and early 21st centuries and (bottom) the early 19th century using Mode-Sim. Green shadings indicate northward flux while purple indicates southward flux. The orange line depicts the energy flux at the equator (right axis, negative values indicate southward flux). Vertical lines in the bottom panel denote years with volcanic eruptions highlighted in Hand et al. (2023).

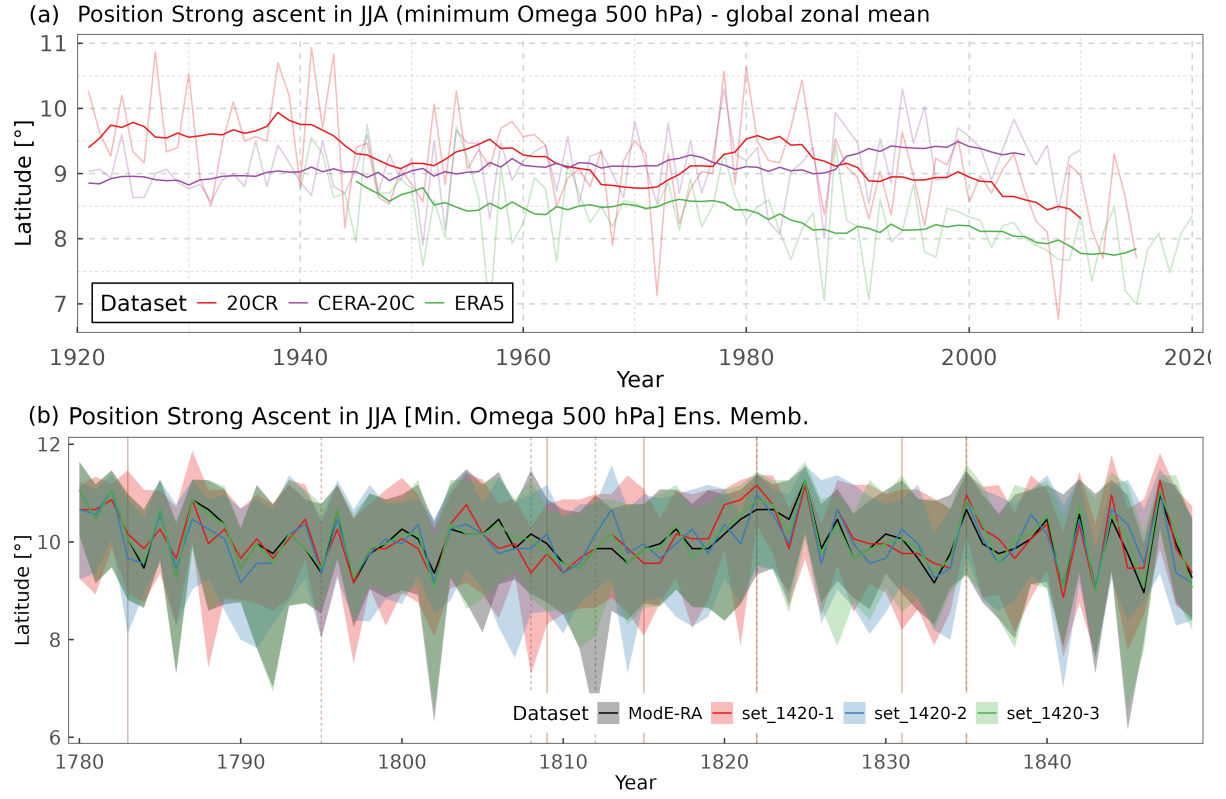


**Figure S3. Global position of the strong ascent of moist air** (Global zonal mean minimum vertical velocity at 500 hPa), for (a) the 20th century and (b) the early 19th century bottom. Colors depict three different reanalyses in the 20th century and the three subsets in the ModE-RA family of reanalyses. In the top panel, tick lines represent the 11-year moving average and the faded lines the annual time series. In the bottom panel, lower and upper ribbon represent the 5 and 95 percentiles ensemble members' spread and tick color line represents the ensemble mean. Vertical lines in the bottom panel denote years with volcanic eruptions highlighted in Hand et al. (2023).

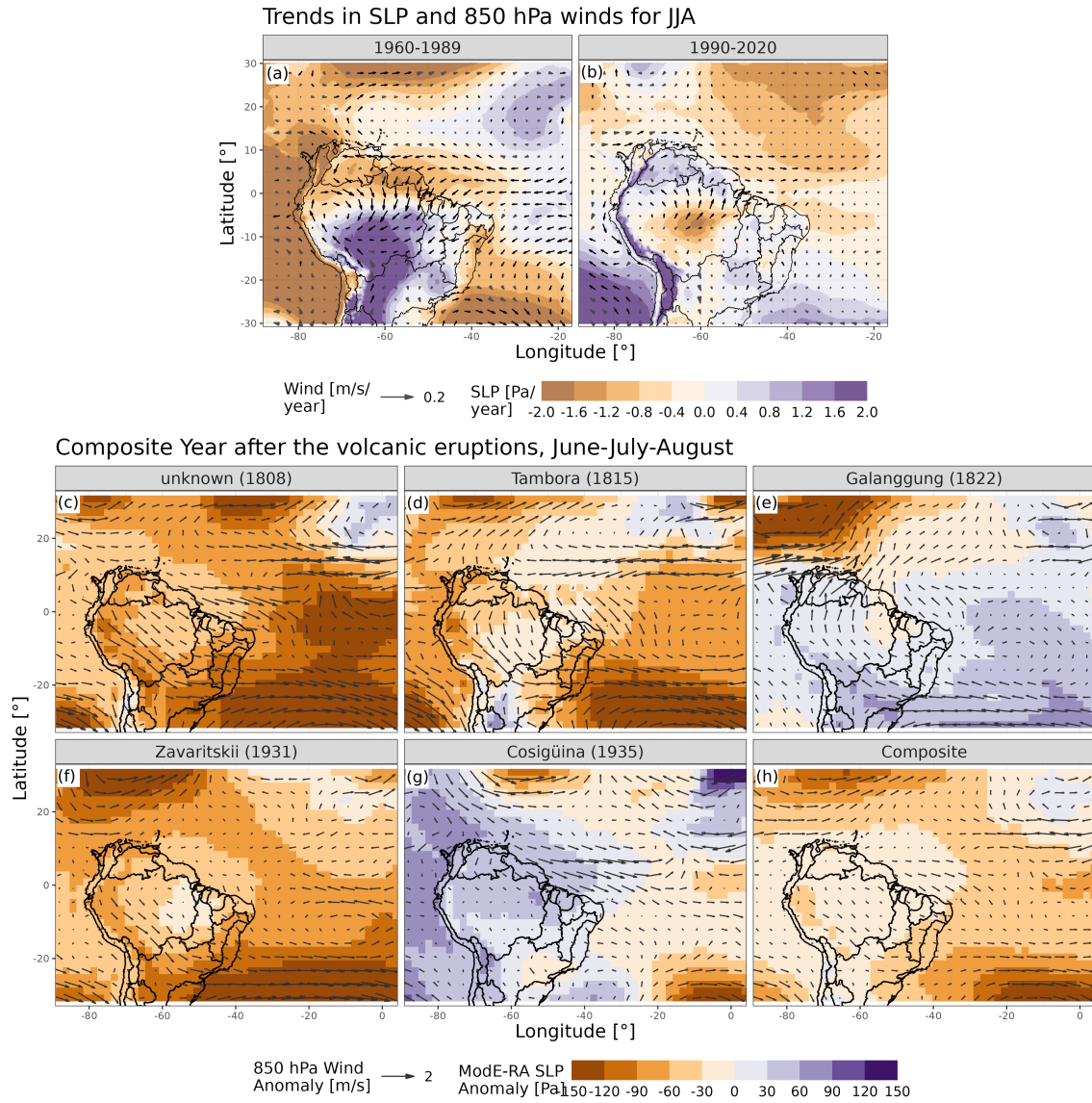


**Figure S4. Changes in sea level pressure and 850 hPa wind** (a) Linear slope coefficients of ERA5 850 hPa wind components (arrows), and Sea Level Pressure (shading) against Gregorian year for the boreal summer -JJA- in the 1960-1989 period. (b) same as (a) but for the period 1990-2020. (c to g) Boreal summer anomalies in the year after the volcanic eruption with ModE-RA wind components (arrows), and ModE-RA Sea Level Pressure (shading). (h) Same as (c) but the composite of the five eruptions.

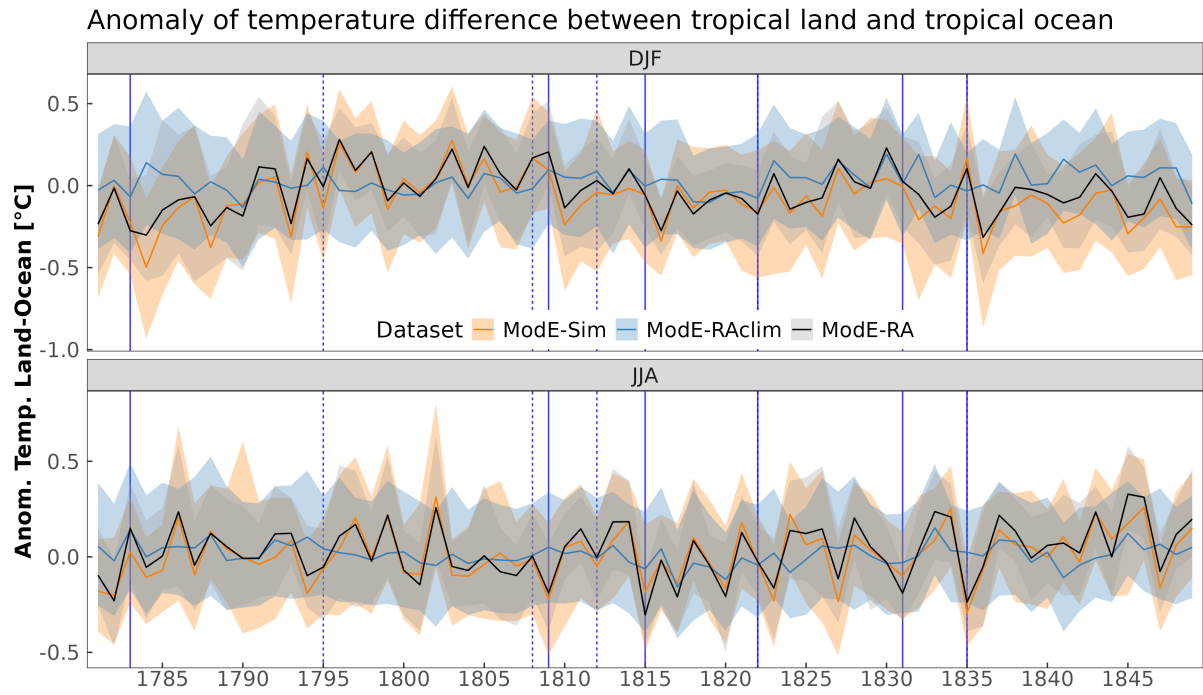


**Figure S5. Early 19th century anomalies of the temperature contrast between the land and the ocean in the tropics for (a) DJF and (b) JJA. Vertical lines display years with volcanic eruptions highlighted in Hand et al. (2023).**